RSC Advances

PAPER

View Article Online
View Journal | View Issue

Open Access Article. Published on 05 January 2017. Downloaded on 10/31/2025 12:55:51 PM.
This article is licensed under a Creative Commons Attribution-NonCommercial 3.0 Unported Licence.

Cite this: *RSC Adv.*, 2017, 7, 6875

Tuning strain and photoluminescence of confined Au nanoparticles by hydrogen passivation

Cailei Yuan,*[a] Yaxing Mei,[a] Ting Yu,[a] Yong Yang,[a] Qinliang li,[a] Aijun Hong,[a] Keng Xu,[a] Xingfang Luo,*[a] Jun He[b] and Wen Lei[c]

Received 29th November 2016
Accepted 4th January 2017

DOI: 10.1039/c6ra27499d

www.rsc.org/advances

Au nanoparticles confined in an Al_2O_3 matrix are synthesized using pulsed laser deposition method and rapid thermal annealing technique. The confined Au nanoparticles experience a compressive strain during the growth process. It is demonstrated that hydrogen passivation can be used to enhance and tailor the optical properties of confined Au nanoparticles by engineering the strain and defect states of the confined Au nanoparticles. The findings provide an insight and useful methodology to improve the emission efficiency of noble metal nanoparticle based materials for potential application in optoelectronic and photonic devices.

Introduction

Recently, the optical properties of noble metal nanoparticles, particularly surface plasmon resonance in the visible region, have attracted significant attention due to the potential applications in optoelectronic and photonic devices.[1–5] Among those noble metal nanoparticles, Au nanoparticles are promising materials for fabricating light emitting devices due to their strong surface plasmonic effect.[6,7] As a result, photoluminescence (PL) of Au nanoparticles has become a focus of study.[8,9] To achieve their final device applications, substantial study has been carried out to understand the light emission process and improve the emission efficiency of Au nanoparticles. For practical device applications, Au nanoparticles are usually embedded in a solid matrix. However, because of the thermal expansion mismatch between Au nanoparticles and the surrounding matrix, substantial strain is generated and accumulated inside and around Au nanoparticles during the growth process.[10,11] The accumulation and relaxation of strain can lead to the generation of defects in the nanoparticles and in the vicinity of the interface between the nanoparticles and the surrounding matrix.[11,12] These bulk and interfacial defects can degrade the physical properties of Au nanoparticles such as carrier lifetime, which can have a disastrous impact on the final device performance.[13] Because of the large surface/volume ratio of nanoparticles, the impact of interfacial defects on the optical properties of Au nanoparticles can be even more significant. Thus, to achieve high performance functioning devices based on confined Au nanoparticles, bulk and interfacial defects as well as their related defect energy states must be eliminated or inactivated.

Passivation provides an effective methodology to eliminate the defect energy states or make them inactive. SiO_2 and Si_3N_4 surface passivation has been widely applied to passivate Si solar cells to achieve high device performance *via* bonding the dangling bonds at the Si semiconductor surfaces.[14,15] Apart from surface passivation, bulk passivation can also help to eliminate the defect energy states in materials. For example, hydrogen atoms have been used to passivate the defects in bulk HgCdTe infrared materials.[16] Hydrogen atoms have also been used to passivate Si nanoparticles, leading to a significant enhancement of the PL emission efficiency by passivating the non-radiative defects at the interface between Si nanoparticles and the surrounding matrix.[17,18] However, little attention has been devoted to enhancing the light emission efficiency of Au nanoparticles. Herein, we present a study on hydrogen passivation of Au nanoparticles embedded in an Al_2O_3 matrix. After hydrogen passivation, the PL emission intensity increased three-fold, which indicates that hydrogen passivation can effectively eliminate or inactivate the defect states in Au nanoparticles.

Experimental

Au nanoparticles confined in an amorphous Al_2O_3 matrix were synthesized using pulsed laser deposition (PLD) method and rapid thermal annealing (RTA) technique. Briefly, a KrF pulsed laser beam with a 248 nm wavelength and a frequency of 10 Hz was used to ablate the target. A part of high-purity (99.99%) circular Al_2O_3 plate (about 40 mm in diameter) and a part of

[a]*Jiangxi Key Laboratory of Nanomaterials and Sensors, School of Physics, Communication and Electronics, Jiangxi Normal University, 99 Ziyang Avenue, Nanchang 330022, Jiangxi, China. E-mail: clyuan@jxnu.edu.cn; xfluo@jxnu.edu.cn*
[b]*Hunan Key Laboratory for Super-micro Structure and Ultrafast Process, School of Physics and Electronics, Central South University, 932 South Lushan Road, Changsha 410083, Hunan, China*
[c]*School of Electrical, Electronic and Computer Engineering, The University of Western Australia, 35 Stirling Highway, Crawley 6009, Australia*

Open Access Article. Published on 05 January 2017. Downloaded on 10/31/2025 12:55:51 PM.
This article is licensed under a Creative Commons Attribution-NonCommercial 3.0 Unported Licence.

high-purity (99.99%) Au square plate (about 8 mm in length) were used as the targets. The deposition of the film on the Si substrate was carried out inside a high-vacuum chamber at a background pressure of about 1×10^{-7} Torr, with the substrate kept at room temperature. After the deposition, the sample was subjected to RTA at 800 °C for 60 s under either pure N_2 or 10% H_2/Ar atmosphere, and the nanoparticles obtained were labeled as nitrogen-annealed or hydrogen-annealed Au nanoparticles. The structure of the deposited film was examined *via* high resolution transmission electron microscopy (HRTEM) with a JEOL 2010 microscope. The TEM electron diffraction pattern was matched against a simulated diffraction pattern generated using the Java Electron Microscopy Simulation (JEMS) software.[10,11] X-ray photoelectron spectroscopy (XPS) measurements were carried out with a Kratos XSAM800 spectrometer using Al Kα radiation. PL and Raman spectroscopy measurements were carried out at room temperature with a HORIBA LabRAM HR Evolution instrument, at an excitation wavelength of 325 nm and 514 nm, respectively.

Results and discussion

Fig. 1(a) shows the HRTEM image of the hydrogen-annealed Au nanoparticles confined in the Al_2O_3 matrix. It can be seen that a large number of Au nanoparticles are formed in the Al_2O_3 matrix. Fig. 1(b) displays the HRTEM image of a single hydrogen-annealed Au nanoparticle confined in the Al_2O_3 matrix. Clearly, the Al_2O_3 matrix still remains amorphous after annealing under hydrogen atmosphere, whereas the Au nanoparticles are crystalline with a spherical shape. The average size of the hydrogen-annealed Au nanoparticles is about 5 nm. Fig. 1(c) shows the electron diffraction pattern of the hydrogen-annealed Au nanoparticles. The diffraction pattern was matched against a simulated diffraction pattern generated *via* the JEMS software. By comparing the experimental diffraction pattern with the simulated one, it could be concluded that the hydrogen-annealed Au nanoparticles have a cubic crystal structure (space group $Fm\bar{3}m$). Fig. 1(d) shows the HRTEM image of a single nitrogen-annealed Au nanoparticle confined in the Al_2O_3 matrix. Similarly, a large number of Au nanoparticles are formed in the Al_2O_3 matrix, and the Al_2O_3 matrix remains amorphous after annealing under nitrogen atmosphere. The average size of the nitrogen-annealed Au nanoparticles was also around 5 nm. Fig. 1(e) presents the HRTEM image of a single nitrogen-annealed Au nanoparticle confined inside the Al_2O_3 matrix. It can be seen that crystalline Au nanoparticles are formed in the Al_2O_3 matrix. Fig. 1(f) shows the electron diffraction pattern of the nitrogen-annealed Au nanoparticles. Similarly, by comparing the experimental diffraction pattern with the simulated one, it could be concluded that nitrogen-annealed Au nanoparticles also have a cubic crystal structure (space group $Fm\bar{3}m$). Therefore, annealing under different atmospheres does not have much of an effect on the crystal structure, size and morphology of the Au nanoparticles confined in the Al_2O_3 matrix.

To confirm the chemical composition of the Au nanoparticles confined in the Al_2O_3 matrix, XPS measurements were performed on the Au nanoparticles annealed as well as on pure bulk Au, for reference. Fig. 2 shows the high-resolution XPS spectra of the Au (4f) peaks for bulk Au, hydrogen-annealed Au and nitrogen-annealed Au nanoparticles confined in the Al_2O_3 matrix. The doublet peaks of Au ($4f_{7/2}$) and Au ($4f_{5/2}$), located at 84.1 and 87.8 eV, respectively, can be clearly observed for bulk Au, which can be attributed to the presence of Au in the metallic state (Au^0).[19] However, four peaks can be clearly observed in the XPS spectrum of the nitrogen-annealed Au nanoparticles. The doublet peaks at 84.1 and 87.8 eV are characteristic for metallic Au. The two very small peaks at 84.9 and 88.6 eV can be assigned to the ionic gold species $Au^{\delta+}$, which is in line with data reported in literature,[20] indicating the existence of bulk and interfacial defects in Au nanoparticles. In contrast, for the hydrogen-annealed Au nanoparticles, only the doublet peaks at 84.1 and

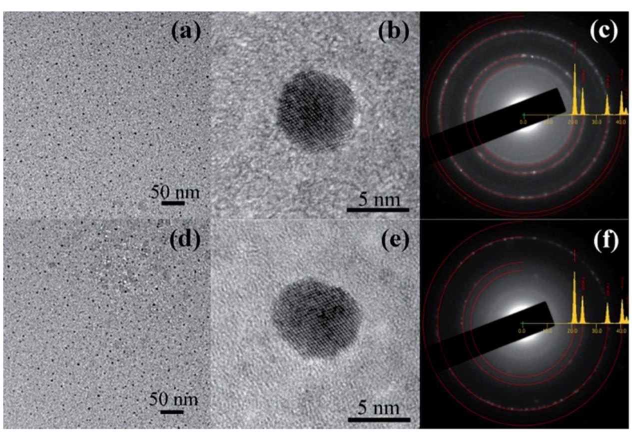

Fig. 1 (a) HRTEM image of hydrogen-annealed Au nanoparticles confined in the Al_2O_3 matrix; (b) HRTEM image of a single hydrogen-annealed Au nanoparticle; (c) electron diffraction pattern of hydrogen-annealed Au nanoparticles; (d) HRTEM image of nitrogen-annealed Au nanoparticles confined in the Al_2O_3 matrix; (e) HRTEM image of a single nitrogen-annealed Au nanoparticle; (f) electron diffraction pattern of nitrogen-annealed Au nanoparticles.

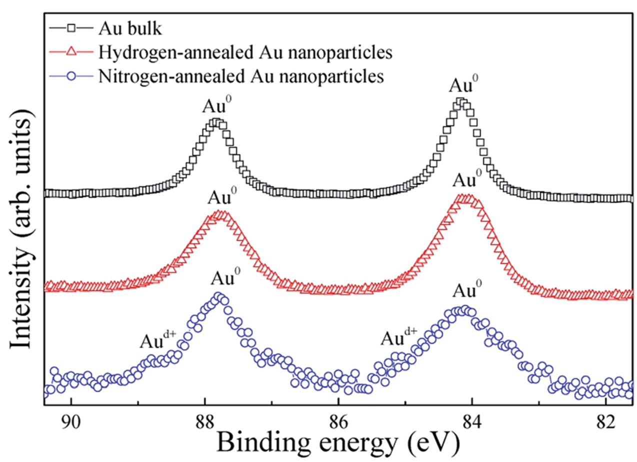

Fig. 2 XPS spectra of Au 4f electrons from Au bulk, hydrogen-annealed and nitrogen-annealed Au nanoparticles confined in the Al_2O_3 matrix.

This journal is © The Royal Society of Chemistry 2017

Open Access Article. Published on 05 January 2017. Downloaded on 10/31/2025 12:55:51 PM.
This article is licensed under a Creative Commons Attribution-NonCommercial 3.0 Unported Licence.

87.8 eV can be observed, which indicates that Au nanoparticles remain in the metallic crystalline phase after annealing. This result clearly demonstrates that hydrogen atoms can bond with the dangling bonds, and thus passivate interfacial defects on the surface of the Au nanoparticles, as well as the defects inside the nanoparticles.

Because of the thermal expansion mismatch between Au nanoparticles and Al_2O_3, the formation and growth of Au nanoparticles in the Al_2O_3 matrix *via* PLD and RTA are accompanied by the generation and accumulation of strain. During the growth process, Au nanoparticles will suffer a substantial compressive strain due to volume expansion whilst confined within the Al_2O_3 matrix. However, strain can have a significant impact on the generation and distribution of defects, and subsequently on the optical properties of Au nanoparticles. Thus, it is essential to have an understanding about the strain and its distribution in Au nanoparticles as well as in the surrounding matrix. In order to understand the strain within the system, the strain distribution in Au nanoparticles confined in the Al_2O_3 matrix was qualitatively simulated using finite element (FE) calculations, which are performed with the commercial ANSYS software package.[10,11] The Young's modulus is taken to be 170 and 360 GPa for Au and Al_2O_3, respectively, while the Poisson's ratio is taken to be 0.42 and 0.24 for Au and Al_2O_3, respectively. Fig. 3(a) shows the cross-sectional strain distribution for a Au nanoparticle grown in an Al_2O_3 matrix. Correspondingly, Fig. 3(b) shows the *X*–*Y* plane strain profile for a Au nanoparticle grown in an Al_2O_3 matrix. As expected, the Au nanoparticle suffers compressive strain from the Al_2O_3 matrix. Moreover, an inhomogeneous strain distribution can be observed, which is denoted by the different colors as labeled by the marks in Fig. 3(a). It can also be observed that the strain at the center of the Au nanoparticle is distributed homogeneously and the strain at the surface of the nanoparticle is weaker than that at the center of the nanoparticles. As a matter of fact, because of the large surface/volume ratio in nanoparticles, the inhomogeneous strain distribution can have a significant impact on interfacial defect states, and consequently on the optical properties of isolated nanoparticles, which will be discussed later.

To further study the strain in Au nanoparticles, Raman spectroscopy measurements were performed on the annealed

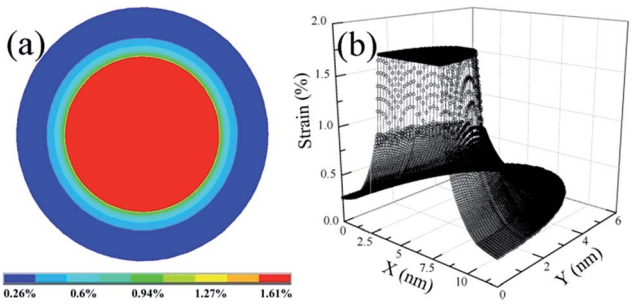

Fig. 3 (a) Cross-sectional strain distribution in a Au nanoparticle confined in an Al_2O_3 matrix; (b) *X*–*Y* plane strain profile of Au nanoparticles confined in an Al_2O_3 matrix.

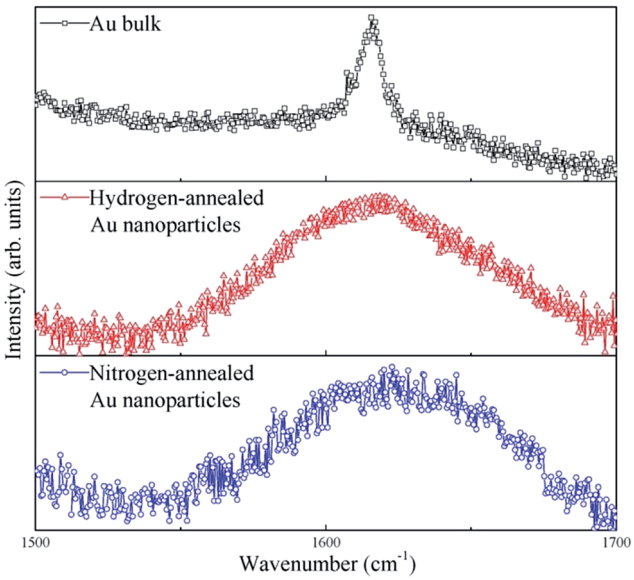

Fig. 4 Raman spectra of bulk Au, hydrogen-annealed and nitrogen-annealed Au nanoparticles excited at a wavelength of 518 nm.

Au nanoparticles as well as on bulk Au, for reference. Fig. 4 displays the room temperature Raman spectra of bulk, hydrogen-annealed and nitrogen-annealed Au nanoparticles excited at a wavelength of 518 nm. A Raman peak centered at about 1615 cm^{-1} can be clearly observed for bulk Au.[21] On the other hand, a Raman peak centered at about 1618 cm^{-1} and 1623 cm^{-1} can be observed for hydrogen-annealed and nitrogen-annealed Au nanoparticles, respectively. The Raman peak of Au nanoparticles confined in Al_2O_3 matrix displays a blue-shift. This clearly demonstrates that Au nanoparticles grown inside an Al_2O_3 matrix are under significant compressive strain,[22,23] which is consistent with the strain simulation results. Moreover, it should also be noted that the peak shift of the nitrogen-annealed Au nanoparticles is larger than that of the hydrogen-annealed Au nanoparticles, which also indicates that the compressive strain in nitrogen-annealed Au nanoparticles is larger than that in the hydrogen-annealed Au nanoparticles. This might be due to the fact that hydrogen atoms can bond with the dangling bonds, and thus passivate interfacial defects on the surface and inside the Au nanoparticles, leading to a relaxation in the network strain. Hydrogen atoms have a smaller volume and higher reactivity than nitrogen atoms; this makes it easier for hydrogen to diffuse into Au nanoparticles and passivate the defects, leading to a dramatic impact on the optical properties of Au nanoparticles.

Fig. 5 shows the PL spectra recorded at room temperature for amorphous Al_2O_3 thin films, hydrogen-annealed and nitrogen-annealed Au nanoparticles confined in an amorphous Al_2O_3 matrix. Clearly, no PL peaks can be observed for the reference amorphous Al_2O_3 thin film. In contrast, a PL band centered at around 585 nm can be clearly observed for samples having Au nanoparticles confined in the amorphous Al_2O_3 matrix. Therefore, the observed PL peak can be attributed to the Au nanoparticles. As can be seen in Fig. 5, the PL peak intensity of the Au

Open Access Article. Published on 05 January 2017. Downloaded on 10/31/2025 12:55:51 PM.
This article is licensed under a Creative Commons Attribution-NonCommercial 3.0 Unported Licence.

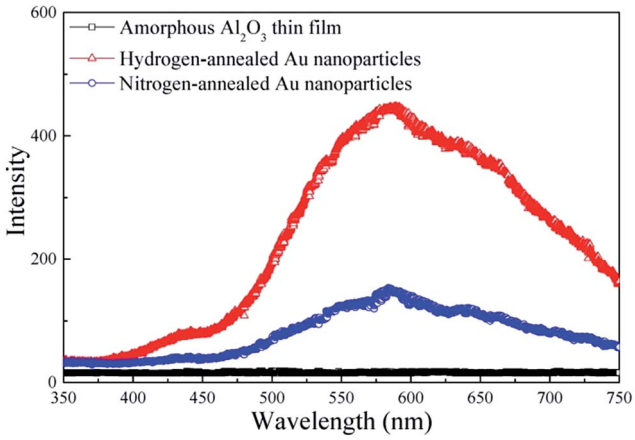

Fig. 5 PL spectra of amorphous Al_2O_3 thin films, hydrogen-annealed Au nanoparticles and nitrogen-annealed Au nanoparticles.

nanoparticles annealed under hydrogen atmosphere is around three times that of Au nanoparticles annealed under nitrogen atmosphere. This is mainly due to the fact that defects in the Au nanoparticles and in the vicinity of Au nanoparticles are effectively passivated by hydrogen atoms, leading to an enhanced light emission efficiency. As discussed previously, when spherical Au nanoparticles are formed in the Al_2O_3 matrix, the matrix exerts an isotropic pressure on the nanoparticles, giving rise to a compressive strain in the Au nanoparticles. The strain and its relaxation could result in several defect states inside the Au nanoparticle and in the vicinity of the interface between Au nanoparticles and Al_2O_3 matrix, ultimately also resulting in several nonradiative surface defects, which can causes low PL emission efficiency for Au nanoparticles.[24] As indicated from the Raman spectra, the compressive strain in the hydrogen-annealed Au nanoparticles was less than that in the nitrogen-annealed Au nanoparticles. Therefore, hydrogen-annealed Au nanoparticles had less defect states. More importantly, annealing under hydrogen atmosphere also allows the hydrogen atoms to passivate the defect states and eliminate the non-radiative defects in the Au nanoparticles,[17] which is consistent with results of the XPS spectra. As a result, the PL emission intensity of hydrogen-annealed Au nanoparticles is effectively enhanced, being almost 3-fold that of nitrogen-annealed Au nanoparticles.

Conclusion

In summary, Au nanoparticles confined in an Al_2O_3 matrix are synthesized using the PLD method and RTA technique. The confined Au nanoparticles experience a compressive strain during the growth process. It is found that annealing under hydrogen atmosphere can relax compressive strain in the Au nanoparticles, and effectively passivate their defect states, leading to an enhanced emission efficiency. The findings presented here provide an insight and offer a useful methodology to enhance the emission efficiency of noble metal nanoparticle-based materials for potential applications in optoelectronic and photonic devices.

Acknowledgements

This study was supported by the Natural Science Foundation of China (Grant No. 51461019, 51661012, 51361013, 51561012 and 61664005), the Project for Young Scientist Training of Jiangxi Province (Grant No. 20153BCB23016), the Natural Science Foundation of Jiangxi Province (Grant No. 20151BAB202004 and 20161BAB201022), and the Australian Research Council (Grant No. FT130101708, DP170104562 and LE170100233).

References

1 H. M. Hiep, H. Yoshikawa, M. Saito and E. Tamiya, *ACS Nano*, 2009, **3**, 446.
2 S. Murai, Y. Fujimoto, K. Iwata, K. Fujita and K. Tanaka, *Appl. Phys. Lett.*, 2011, **98**, 121917.
3 K. M. Guo, M. Y. Li, X. L. Fang, X. L. Liu, B. Sebo, Y. D. Zhu, Z. Q. Hu and X. Z. Zhao, *J. Power Sources*, 2013, **230**, 155.
4 Z. B. Zhan, R. Xu, X. Z. Zheng, Q. Fu, M. H. Wu and Y. Lei, *Nanotechnology*, 2016, **27**, 445301.
5 V. Garg, B. S. Sengar, V. Awasthi, Aaryashree, P. Sharma, C. Mukherjee, S. Kumar and S. Mukherjee, *RSC Adv.*, 2016, **6**, 26216.
6 Y. H. Lee, D. H. Kim, K. H. Yoo and T. W. Kim, *Appl. Phys. Lett.*, 2014, **105**, 183303.
7 D. H. Kim and T. W. Kim, *Org. Electron.*, 2016, **34**, 270.
8 Y. Ishida, T. Sumi and T. Yonezawa, *New J. Chem.*, 2015, **39**, 5895.
9 J. Prakash, V. Kumar, R. E. Kroon, K. Asokan, V. Rigato, K. H. Chae, S. Gautam and H. C. Swart, *Phys. Chem. Chem. Phys.*, 2016, **18**, 2468.
10 C. L. Yuan, Z. X. Jiang and S. L. Ye, *Nanoscale*, 2014, **6**, 1119.
11 C. L. Yuan, Y. Zhang, J. He, S. L. Ye, W. Lei, X. S. Liu and G. Gu, *J. Mater. Chem. C*, 2014, **2**, 8768.
12 Z. X. Jiang, C. L. Yuan and S. L. Ye, *RSC Adv.*, 2014, **4**, 19584.
13 J. Xu, J. Moxom, B. Somieski, C. W. White, A. P. Mills, R. Suzuki and S. Ishibashi, *Phys. Rev. B: Condens. Matter Mater. Phys.*, 2001, **64**, 113404.
14 K. Watanabe, R. Tsuchiya, T. Mine, Y. Yonamoto, N. Akamatsu and M. Hatano, *Appl. Phys. Lett.*, 2012, **101**, 153902.
15 C. A. Lin, K. Y. Lai, W. C. Lien and J. H. He, *Nanoscale*, 2012, **4**, 6520.
16 W. D. Hu, X. S. Chen, Z. H. Ye and W. Lu, *Appl. Phys. Lett.*, 2011, **99**, 091101.
17 S. Cheylan and R. G. Elliman, *Appl. Phys. Lett.*, 2001, **78**, 1225.
18 S. P. Withrow, C. W. White, A. Meldrum, J. D. Budai Jr, D. M. Hembree and J. C. Barbour, *J. Appl. Phys.*, 1999, **86**, 396.
19 J. H. Liu, G. Liu, C. Liu, W. X. Li and F. Wang, *Catal. Sci. Technol.*, 2016, **6**, 2055.
20 D. A. Bulushev, I. Yuranov, E. I. Suvorova, P. A. Buffat and L. Kiwi-Minsker, *J. Catal.*, 2004, **224**, 8.
21 Q. Fu, K. M. Wong, Y. Zhou, M. H. Wu and Y. Lei, *RSC Adv.*, 2015, **5**, 6172.
22 M. Montazeri, M. Fickenscher, L. M. Smith, H. E. Jackson, J. Yarrison-Rice, J. H. Kang, Q. Gao, H. H. Tan, C. Jagadish,

 This journal is © The Royal Society of Chemistry 2017

Open Access Article. Published on 05 January 2017. Downloaded on 10/31/2025 12:55:51 PM.
This article is licensed under a Creative Commons Attribution-NonCommercial 3.0 Unported Licence.

Y. N. Guo, J. Zou, M. E. Pistol and C. E. Pryor, *Nano Lett.*, 2010, **10**, 880.
23 Q. Wang, Y. X. Gao, G. M. Mao, H. Liu and X. M. Ren, *Appl. Phys. Lett.*, 2015, **107**, 082108.
24 L. Ravelli, C. Macchi, S. Mariazzi, P. Mazzoldi, W. Egger, C. Hugenschmidt, A. Somoza and R. S. Brusa, *J. Phys. D: Appl. Phys.*, 2015, **48**, 495302.